Hyperpolarized (3)He apparent diffusion coefficient MRI of the lung: Reproducibility and volume dependency in healthy volunteers and patients with emphysema.

Diaz, Sandra; Casselbrant, Ingrid; Piitulainen, Eeva; Pettersson, Göran; Magnusson, Peter; Peterson, Barry; Wollmer, Per; Leander, Peter; Ekberg, Olle; Åkeson, Per

Published in:
Journal of Magnetic Resonance Imaging

DOI:
10.1002/jmri.21212

2008

^{3}He apparent diffusion coefficient MRI of the lung: Reproducibility and volume dependency in healthy volunteers and patients with emphysema

Sandra Diaz, MD[1], Ingrid Casselbrant, MD[2], Eeva Piitulainen, MD PhD[2], Goran Pettersson, PhD[3], Peter Magnusson, PhD[3], Barry Peterson, PhD[4], Per Wollmer MD PhD[5], Peter Leander MD PhD[1], Olle Ekberg MD PhD[1] and Per Akeson MD PhD[1].
[1]Dept of Radiology, Malmö University Hospital, Malmö, Sweden; [2]Dept of Respiratory Medicine, Malmö University Hospital, Malmö, Sweden; [3]GE Healthcare, Malmö, Sweden; [4]Pfizer, USA; [5]Dept of Clinical Physiology, Malmö, Sweden.

Sandra Diaz, MD
Department of Clinical Sciences, Malmö and Lund
S. Förstadsgatan 101, Ing 44
SE-205 02 Malmö, Sweden
Phone: +46-(0)-40-33 87 96
Fax: +46-(0)-40- 33 87 98
E-mail: Sandra.diaz@med.lu.se

Hyperpolarized gases, Reproducibility

ABSTRACT

PURPOSE: To measure the apparent diffusion coefficient (ADC) of hyperpolarized (HP) ^{3}He gas using diffusion weighted MRI in healthy volunteers and patients with emphysema and examine the reproducibility and volume dependency.

MATERIALS AND METHODS: Eight healthy volunteers and sixteen patients with emphysema were examined after inhalation of HP ^{3}He-gas mixed with nitrogen (N_2) during breath-hold starting from functional residual capacity (FRC) in supine position. Coronal diffusion-sensitized MR images were acquired. Each subject was imaged on three separate days over a 7-day period and received two different volumes (6% and 15% of total lung capacity, TLC) of HP ^{3}He each day. ADC maps and histograms were calculated. The mean and standard deviation (SD) of the ADC at different days and volumes were compared.

RESULTS: The reproducibility of the mean ADC and SD over several days was good in both healthy volunteers and patients (SD range of 0.003-0.013 cm^2/s and 0.001-0.009 cm^2/s at 6% and 15% of TLC for healthy volunteers, and a SD-range of 0.001-0.041 cm^2/s and 0.001-0.011 cm^2/s respectively for patients). A minor but significant increase in mean ADC with increased inhaled gas volume was observed in both groups.

CONCLUSION: Mean ADC and SD of HP ^{3}He MRI is reproducible, discriminates well between healthy controls and patients with emphysema at the higher gas volume. This method is robust and may be useful to gain new insights into the pathophysiology and course of emphysema.

Key Words: hyperpolarized; helium-3; ADC; MRI; lungs; reproducibility

INTRODUCTION

The habit of smoking is increasing worldwide and so is one of its direct consequences, *i.e.* the chronic obstructive pulmonary disease (COPD). By the year 2020 COPD is expected to rank third as a cause of mortality and fifth of morbidity (1). A validated imaging technique that is sensitive to very early structural changes in the lungs could be helpful in the design of therapy and management of emphysema.

Magnetic resonance imaging (MRI) using hyperpolarized (HP) gases as helium (^{3}He) have emerged as a promising technique for studies of the structure and function of the lungs. Inhalation of HP ^{3}He can be used not only to derive information related to regional ventilation but also to the size of the alveoli. This is accomplished by measurement of the apparent diffusion coefficient (ADC) of inhaled HP ^{3}He. When HP ^{3}He is inhaled, diffusion of the gas is restricted by the boundaries of the alveoli and if restricted diffusion measurement conditions are met, the measured ADC will reflect the size of the peripheral airway spaces (2,3,4). It could thereby allow quantification of the structural changes (of the lungs) in emphysema. The ADC has been shown to increase in animals with elastase-induced emphysema (5). Studies have also been performed in small numbers of healthy adult subjects and subjects with lung disease (6-12). In these studies, the ADC values in emphysematous lungs were increased relative to ADC values obtained in subjects with healthy lungs.

The mean ADC of gases such as helium, measured during breath hold, is expected to be dependent on the lung volume reached after inhalation of the gas. It has been demonstrated (11,12) that there is a significant gradient in alveolar size, as a function of posture, with measurements of ADC HP ^{3}He-gas. However, no systematic information is available about the dependency of the ADC for ^{3}He on lung volume.

Measurement of the ADC for ^{3}He is non-invasive and does not entail exposure of ionizing radiation. It may therefore be a suitable technique for monitoring of the progression of emphysema. This requires the reproducibility of the technique to be known.

The aims of this study were to assess the values, the reproducibility of the ADC measurement in volunteers and patients with mild to moderate emphysema, to study the dependency of the ADC on inhaled volume of gas and to confirm the gravity effect in lung physiology.

MATERIALS AND METHODS

Subjects

Two different populations were included: one group of 8 healthy volunteers (3 men, 5 women; age range 40-60 years) with normal physical examination results, no smoking during the last five years and no more than a 5 pack-year smoking history, pulmonary function test with FEV_1 > 80% of predicted normal value and FEV_1 /FVC >70%. The patient group, in total 16 patients, consisted of 2 subgroups: eight patients with emphysema due to alpha-1 antitrypsin deficiency (AATD), phenotype PiZ (5 men, 3 women; age range 30-70 years), with FEV_1 50% to 80% of predicted normal value and FEV_1 /FVC < 70% and eight patients with usual COPD emphysema phenotype PiM (2 man, 6 women; age range 40-60 years) with FEV_1 50% to 70% of predicted normal values and FEV_1 /FVC < 70% after use of bronchodilator.

Exclusion criteria were respiratory illness within 6 weeks before study inclusion, history of asthma or allergy and standard MRI contraindications.

All subjects underwent PFT performed according to the Guidelines of the European Respiratory Society (13). The inclusion criteria were followed strictly and patients with mild to moderate emphysema could thereby be enrolled. Each subject visited the center for a screening visit and three imaging visits separated by 1 to 7 days. At all visits the following examinations were performed: spirometry, 12 lead ECG, vital signs (blood pressure, heart rate, respiratory rate, oxygen saturation and body temperature). In the patient group concomitant medications were administered as usual, except for lung disease medication, which was adjusted to allow performance of FEV_1 reversibility test using 0.4 mg salbutamol during the screening visit.

Heart rate, lead II ECG, oxygen saturation and blood pressure were continuously monitored during imaging using a Maglife C Plus (Schiller AG, Switzerland). A pulmonologist supervised all studies.

The ethics committee approved the study and the investigation conformed to the principles outlined in the Declaration of Helsinki.

^{3}He polarization procedure

Polarization of the ^{3}He gas was performed with a prototype commercial polarizer (IGI.9600.He, GE Healthcare, Durham, NC, USA) with use of the method of collisional spin exchange between laser-polarized rubidium vapour and ^{3}He (14). The polarization process was started in the afternoon the day before imaging, and the polarization process was terminated about 30 min before the subject was imaged. The polarizer produced approx. 1 bar·liter with a polarization of 35–45% during the over-night runs. The polarized ^{3}He gas was dispensed into 1-2 liter Tedlar bags (Jensen Inert, Coral Springs, FL, USA), mixed with nitrogen (N_2) to obtain a volume. At either 6% or 15% of total

lung capacity (TLC) the gas was then carried to the MR imager (1–2 min transportation time).

^{3}He administration

Each subject was imaged on 3 separated days during a 7-day period and received two volumes of HP ^{3}He during on each of the three imaging days with one volume being 6% and the other 15% of TLC. All volumes had a planned net concentration of 4.5 mmol-hyperpolarized ^{3}He but different volumes of filler gas (N_2). The gas was administered in the supine position by instruction the subject to inhale from functional residual capacity (FRC) until the bag was empty. There were at least 5 but not more than 10 minutes between the doses.

MR imaging was performed using a 1.5 T whole body MR scanner (Siemens Magnetom Sonata, software: syngo MR 2002 B; Siemens Medical Solutions, Erlangen, Germany). Prior to ^{3}He imaging and after inhalation of 500 ml of room air starting from FRC, a coronal proton localizer was acquired during breath-hold using a 2D gradient echo pulse sequence (body coil, TR/TE 160/4.4 ms, flip angle 7°, bandwidth 180 Hz/pixel, FOV 400x400 mm, matrix 119x192, slice thickness 10 mm, interslice distance 1 mm, No. of slices 19, acquisition time 14 sec).

Before ^{3}He imaging, the ^{3}He frequency and the transmitter voltage were adjusted as required for a flip angle of 7°, as used by the pulse sequence for ^{3}He ADC imaging. The ^{3}He frequency was adjusted by acquiring a non-localized free induction decay (FID) during a short breath-hold and after inhalation of a small volume of ^{3}He. The transmitter voltage was adjusted by a FID-acquisition repeated three times during breath-hold after inhalation of the gas remaining after the frequency adjustment. The transmitter voltage

required for a 7° flip angle was calculated by fitting the signal attenuation equation to the measured signal amplitudes from repeated FID-acquisitions.

A diffusion weighted 2D gradient echo sequence (helium body coil, TR/TE 9.6/5.9 ms, flip angle 7°, bandwidth 250 Hz/pixel, FOV 382x470 mm, matrix 80x128 coronal slices, slice thickness 15 mm, inter slice distance 5 mm, No. of slices 10, time of acquisition 15 sec) was used for HP ^{3}He ADC MR imaging. Two images were acquired at each slice position, one without (b0) and one with (b1) a bipolar diffusion sensitizing gradient waveform (b1 = signal attenuation constant =1.6 s/cm^2) applied in the slice direction (b1) with interleaved phase encoding. The coronal slices covered the whole lungs from anterior to posterior. The b0 images were used as ventilation images. A flexible quadrature vest coil (Clinical MR Solutions, LLC, USA) was used for all ^{3}He scanning. The Helispin® Workstation software (GE Healthcare) was used for post processing. An ADC map was calculated from each pair of b0- and b1- images on a pixel-by-pixel basis. A linear least square fit to the natural log of the signal amplitude versus the b-value (b0=0 s/cm^2 and b1=1.6 s/cm^2) was applied. Background pixels were excluded from the ADC calculation using a threshold of 5 times the true standard deviation (SD) in a background region. This SD was obtained by dividing the background mean by 1.253 (14,16).

To eliminate bias from ADC calculated in the large airways, the trachea and main bronchi were manually segmented from the ADC-maps before analysis by an experienced radiologist. ADC maps and frequency distributions (No. of voxels versus ADC values) were calculated for individual slices and the whole lungs. The mean ADC and the standard deviation (SD) were assessed from the ADC-map of each slice. These are called the slice mean ADC and SD. Covering all slices, the total volume mean ADC and SD for each inhaled volume was also calculated. These are called the volume mean ADC and SD. The overall mean ADC and SD per subject were calculated as averages of

the volume mean ADC of the three imaging days. These are called overall mean ADC and SD. The SD of the overall mean ADC was used as a measure of the reproducibility over the three imaging days. Group mean ADC and SD were calculated from the volume mean ADC and SD values for each imaging day for volunteers and patient groups. These data was calculated separately for the 6% and the 15% of TLC volume.

In order to achieve an anterior-posterior distribution of the ADC we calculated for the 15% volume the ADC gradient between the most anterior and the most posterior slice for each subject. This was done by subtracting the mean ADC value of the posterior slice from the value of the anterior slice excluding those slices containing less than 100 voxels.

Statistical analysis

Statistical analysis was performed using SAS® software. The results from the mean ADC measurements across all lung slices for each subject, day and volume inhaled were analyzed using a mixed model repeated-measures analysis of variance. This mixed model utilized subjects as a random effect and day, volume and day-by-volume interaction as fixed effects. The volume (6% and 15%) administered was calculated as a percentage of TLC for each subject. The analysis was used to test for an overall difference among the volume, day, and volume-by-day interaction. The interaction term indicated the reproducibility of the administration of each given volume over time. Assuming no significant interaction existed, simultaneous 95% confidence intervals were constructed on adjusted mean of ADC by imaging day and on all pair wise differences of the mean ADC between imaging day across volumes.

RESULTS

Both planned volumes were administered to all subjects. No serious adverse events were registered.

Reproducibility

Group mean ADC and SD at 6% and 15% of TLC by day and group and the group mean ADC and SD for the combined patient group are shown in Table 1. There was a clear discrimination between healthy volunteers and patients at both volumes at all imaging days. The findings at 15% of TLC are shown in Fig 1.

The overall mean ADC in each subject (mean value of three measurements) at both volumes shows a small intra-individual difference with low SD for all subjects. In the healthy group the SD range was 0.003-0.013 cm^2/s and 0.001-0.009 cm^2/s at 6% and 15% of TLC, respectively. For the patient group the SD-range was 0.001-0.041 cm^2/s and 0.001-0.011 cm^2/s at 6% and 15% of TLC, respectively (Table 2).

The inter-individual difference in overall mean ADC per subject in the healthy group was small both at 6% and 15% of TLC with a range from 0.184 to 0.234 cm^2/sec (inter-individual SD 0.020) and from 0.193 to 0.247 cm^2/sec (inter-individual SD 0.021) respectively (Table 2).

The mixed model analysis (dependence of mean ADC on day, volume and day-by-volume) did not show any statistically significant day or day-by-volume effects on the overall mean ADC and SD per subject (Table 3).

The frequency distributions of the mean ADC showed almost identical curves from day to day in both volunteers and patients and a clear difference between the healthy volunteers and the patients was seen (Fig 2).

Volume

Concerning the effect of inhaled volume on the mean ADC value, the group mean was 0.210 cm^2/s for the 6% volume and 0.218 cm^2/s for the 15% volume in healthy volunteers and 0.381 and 0.387 cm^2/s, respectively, in patients (Table 2).

The statistical analysis of effect using the mixed model showed that there was a small but statistically significant volume effect on the overall mean ADC ($p=0.0014$ in healthy volunteers and $p=0.0265$ in the patient group) as well as a statistically significant volume effect between both volumes (6% and 15% of TLC) on the SD of the mean ADC ($p=0.0032$ in healthy volunteers and $p= 0.068$ in the patient group) (Table 3).

More voxels were seen in the ADC maps at 15% of TLC volume (Table 2). This was especially apparent in one patient who showed a new population of voxels in the frequency distribution at the larger volume (Fig 3).

Antero-posterior distribution

In healthy volunteers an anterior-posterior ADC gradient was found (Table 4). In supine position the mean ADC was higher in anterior than posterior slices with a mean change of 31.1±7.9% at the 15% dose. There was no gradient between the anterior and posterior slices in the patient groups (Table 5).

DISCUSSION

HP ^{3}He MRI is sensitive to regional changes in the structure and morphology of distal airways and alveoli as has been previously demonstrated (3, 17-19). A significant correlation between morphometric measurements and ADC has also been demonstrated in animals (4). However, reproducibility has to be validated in both healthy volunteers

and patients if the method should come into clinical use or be used in longitudinal studies i.e. to assess the effect of new drug therapies designed to monitor changes in the progression of emphysema.

The reproducibility of the mean ADC measurement within a subject is affected by the ability of the subject to lie still, to inhale the whole volume and to hold the breath during imaging. The good reproducibility in this study may in part have been due to our efforts to explain the procedure and train the subjects to cooperate and their success at following the protocol exactly. The results were also similar in an exploratory study (11) where the subjects did not leave the scanner between the imaging sessions. It has also been shown that different centers can achieve comparable results (20).

The slices did not cover the entire lung in all cases. Therefore, the overall day-to-day reproducibility could have been affected by difficulties in positioning the slices at the same location each day. One way to avoid such repositioning errors would be to use a sequence with better volume coverage instead of the 2D sequences used in the present study, and an optimized 3D sequence may be better in this respect. A 3D-sequence could also allow for smaller voxels (21).

However, even with the shortcomings of our study the measurements of mean ADC were very reproducible.

The clear difference in ADC values between volunteers and patients and the lack of overlap between the groups would suggest that ADC values no higher than 0.25-0.27 cm^2/sec should be expected in healthy lungs at an inhaled volume of 15% of TLC. This is in the same range as values from other studies (5, 8, 11, 22) with different diffusion gradients and volumes. However, other factors might influence the normal value, for example age.

It is also important to note that there was a statistically significant dependency on the inhaled volume. The difference found in ADC after inhalation of the two volumes can be related to the expected change in mean radius of the alveoli. FRC was measured in the supine position in the subjects. Moving from the upright to the supine position reduces FRC by 28 % in normal subjects (23). By correcting for position and adding 6 and 15 % of the mean measured TLC in the normal subjects, we obtain the absolute lung volumes. Assuming spherical shape of the alveoli, the ratio between the mean alveolar radius at the two volumes will be the cubic root of the ratio between the volumes. This ratio comes to 0.944, which compares reasonably well to the ratio of the mean ADC of 0.963, given the assumptions.

One other important point is that the method is robust also when areas of the lung are less well ventilated. Even when only a small amount of HP ^{3}He reached an area and the signal therefore was low, we obtained a measurable ADC-value although with higher SD. The SD range at 6% of TLC was higher in both volunteers and patients, than at 15% of TLC (Table 2). The reproducibility was also better at the larger volume with lower intra-individual SDs (Table 2), especially the AATD patients.

In one patient a new population of voxels showed up when the higher volume was used (Fig 3). As seen in the images of this patient, this depended on the fact that the lower lobes were not reached by the gas at the lower volume.

These findings suggest that even though the effect of lung volume on mean ADC is small, the larger volume is preferable because it was well tolerated, provided better reproducibility within subjects and should provide less risk of areas of the lung not being reached by the gas. However, whether or not the 15% of TLC volume is optimal in patients with more severe disease is still to be pursued.

In the supine position an anterior-posterior ADC gradient was found in normal subjects. A gradient in alveolar expansion in the direction of gravity has previously been demonstrated with direct methods (24,13). We found the gradient to be smaller at the higher lung volume, which is in agreement with measurements made with computed tomography (25). However, we did not found an anterior-posterior gradient in the patient groups. We assume that it is because of emphysema changes. The presences of spread destroyed areas, with no special predilection, in the lung parenchyma, make enormous variation of higher ADC values in different regions of the lungs.

In conclusion, ADC measurement with HP 3He MRI is highly reproducible, sensitive to small differences in alveolar size and clearly separates volunteers and patients with mild to moderate emphysema. Dependency on inhaled volume was shown and the higher volume, 15% of TLC, seemed preferable. The method might be a useful tool to gain new insight in the pathophysiology and course of emphysema.

ACKNOWLEDGMENTS

Authors thank Curt Johansson, MSc, Isabella Björk, MSc, Georg Hansson, MSc, Harvey Fountaine, BA and Sven Månsson, PhD for their valuable assistance.

REFERENCES

1. Gulsvik A. The global burden and impact of chronic obstructive pulmonary disease worldwide. Monaldi Arch Chest Dis. 2001 Jun;56(3):261-264.
2. Chen XJ, Möller HE, Chawla MS, Cofer GP, Driehuys B, Hedlund LW, Johnson GA. Spatially resolved measurements of hyperpolarized gas properties in the lung in vivo. Part I: Diffusion coefficient. Magn Reson Med 1999;42:721-728.
3. Yablonskiy DA, Sukstanskii AL, Leawoods JC, Gierada DS, Bretthorst GL, Lefrak SS, Cooper JD, Conradi MS. Quantitative in vivo assessment of lung microstructure at the alveolar level with hyperpolarized ^{3}He diffusion MRI. Proc Natl Acad Sci 2002;99:3111-3116.
4. Peces-Barba G, Ruiz-Cabello J, Cremillieux Y, Rodriguez I, Dupuich D, Callot V, Ortega M, Rubio Arbo ML, Cortijo M, Gonzalez-Mangado N: Helium-3 MRI coefficient: correlation to morphometry in a model of mild emphysema. Eur Respir J 2003;22:14-19.
5. Chen XJ, Hedlund LW, Chawla MS, Möller HE, Johnson GA. Detection of elastase-induced emphysema in rat lungs by measuring diffusion of hyperpolarized ^{3}He. In: Proc Intl Soc Magn Reson Med 7th Meeting, 1999;130.
6. Salerno M, Brokeman JR, de Lange EE, Knight-Scott J, Mugler III JP. Detection of regional microstructural changes of the lung in emphysema using hyperpolarized ^{3}He diffusion MRI. In: Proc Intl Soc Magn Reson Med 8th Meeting, 2000;9.
7. Salerno M, de Lange EE, Altes TA, Truwit JD, Brookeman JR, Mugler III JP. Emphysema: Hyperpolarized helium-3 diffusion MR imaging of the lungs compared with spirometric indexes-initial experience. Radiology 2002;222:252-260.
8. Saam B, Yablonskiy DA, Kodibagkar VD, et al. MR imaging of diffusion of ^{3}He gas in healthy and diseased lungs. Magn Reson Med 2000;44:174-179.

9. Mugler III JP, Brookeman JR, Knight-Scott J, Maier T, de Lange EE, Bogorad PL. Regional measurement of the ^{3}He diffusion coefficient in the human lung. In: Proc Intl Soc Magn Reson Med 7th Meeting 1998:1906.
10. Saam BT, Yablonskiy DA, Gierada DS, Cooper JD, Conradi MS. Measurements of ^{3}He diffusivity in human lung: preliminary results from emphysema patient. In: Proc Intl Soc Magn Reson Med 7th Meeting 1999;136.
11. Morbach A, Gast K, Schmiedeskamp J, Dahmen A, Herweling A, Heussel C, Kauczor H-U, Schreiber W. Diffusion-weighted MRI of the lung with hyperpolarized helium-3: A study of reproducibility. Journal of Magnetic Resonance Imaging 2005;21:765-774.
12. Salerno M, Altes TA, Mugler III JP, Nakatsu M, Hatabu H, de Lange EE: Hyperpolarized noble gas MR imaging of the lung: Potential clinical applications. Eur J Radiol 2001;40:33-44.
13. Siakafas NM, Verniere P, Pride NB, et al. Optimal assessment and management of chronic obstructive pulmonary disease (COPD). The European Respiratory Society Task Force. Eur Respir J 1995;8:1398-1420.
14. Happer W, Miron E, Schaefer S, Schreiber D, van Wijngaarden WA, Zeng X. Polarization of nuclear spins of noble gas atoms by spin exchange with optically pumped alkali-metals atoms. Phys rev A 1984;29:3092-3110.
15. Edelstein WA, Bottomley PA, Pfeifer LM. A signal-to-noise calibration procedure for NMR imaging systems. Med Phys 1984;11:180-185.
16. Henkelman RM. Measurement of signal intensities in the presence of noise in MR images. Med Phys 1985;12:232-233.

17. Tooker Angela C, Hong KS, McKinstry EL, Costello P, Jolesz FA, Albert MS. Distal airways in humans: Dynamic hyperpolarized ^{3}He MR imaging-Feasibility. Radiology 2003;227:575-579.
18. Kauczor HU, Hanke A, van Beek EJR. Assessment of lung ventilation by MR imaging: current status and future perspectives. Eur Radiol 2002;12:1962-1970.
19. Kauczor HU, Eberle B. Elucidation of structure-function relationships in the lung: contributions from hyperpolarized ^{3}helium MRI. Clin Physiol & Func Im 2002;22:361-369.
20. Schreiber WG, Morbach AE, Stavngaard T, Gast KK, Herweling A, Sögaard LV, et al. Resp Physiol Neurobiol 2005 Aug 25;148(1-2):23-42.
21. Wild JM, Woodhouse N, Paley MNJ, Fichele S, Said Z, Kasuboski L, van Beek EJR. Comparison between 2D and 3D gradient-echo sequences for MRI of human lung ventilation with hyperpolarized ^{3}He. Magn Reson Med 2004;52:673-678.
22. Swift AJ, Wild JM, Fichele S, et al. Emphysematous changes and normal variation in smokers and COPD patients using diffusion ^{3}He MRI. Eur J Radiol. 2005 Jun;54(3):352-358.
23. Lumb AB, Nunn JF. Respiratory function and ribcage contribution to ventilation in body positions commonly used during anesthesia. Anesth Analg 1991;73(4):422-426.
24. Glazier JB, Hughes JM, Maloney JE, West JB. Vertical gradient of alveolar size in lungs of dogs frozen intact. J Appl physiology 1967;23(5):694-705.
25. Wollmer P, Albrechtsson U, Brauer K, Eriksson L, Jonsson B, Tylen U. Measurement of pulmonary density by means of X-ray computerized tomography. Relation to pulmonary mechanics in normal subjects. Chest 1986;90(3):387-391.

Table 1. Group Mean and SD at two different volumes.

	Group Mean ADC[1] ± SD[2] at 6% of TLC[3] (cm^2s)			Group Mean ADC ± SD at 15% of TLC (cm^2s)		
	Day 1	Day 2	Day 3	Day 1	Day 2	Day 3
Healthy	0.213 ±0.018	0.211 ±0.021	0.206 ±0.021	0.218 ±0.019	0.219 ±0.022	0.218 ±0.024
COPD[4]	0.338 ±0.055	0.337 ±0.052	0.335 ±0.050	0.336 ±0.052	0.325 ±0.034	0.339 ±0.052
AATD[5]	0.433 ±0.049	0.428 ±0.050	0.413 ±0.048	0.437 ±0.053	0.440 ±0.053	0.439 ±0.057
All Patients	0.385 ±0.070	0.382 ±0.068	0.374 ±0.062	0.386 ±0.072	0.383 ±0.074	0.389 ±0.074

[1]ADC: apparent diffusion coefficient. [2]SD: standard deviation. [3]TLC: total lung capacity.[4] COPD: chronic obstructive lung disease. [5]AATD: alpha-1 antitrypsine deficiency.

Subject/age (y)/ sex/status	FEV_1 (% predicted)	FEV_1/FVC	Overall mean ADC per subject ± SD at 6% of TLC (cm^2/s)	Nr of voxels per subject at 6% of TLC	Overall mean ADC per subject ± SD at 15% of TLC (cm^2/s)	Nr of voxels per subject at 15% of TLC
1/44/M Healthy	93	84	0.194 ± 0.004	17544	0.195 ± 0.002	21453
2/42/M Healthy	130	86	0.229 ± 0.006	19037	0.246 ± 0.004	23444
3/42/F Healthy	92	77	0.184 ± 0.003	13781	0.193 ± 0.006	17477
4/53/F Healthy	107	81	0.229 ± 0.003	12134	0.229 ± 0.004	15194
5/40/F Healthy	105	79	0.191 ± 0.013	18980	0.202 ± 0.001	22698
6/45/F Healthy	105	73	0.216 ± 0.004	19091	0.219 ± 0.003	22047
7/41/F Healthy	119	87	0.204 ± 0.006	18648	0.211 ± 0.001	21228
8/54/M Healthy	111	79	0.234 ± 0.003	18754	0.247 ± 0.009	21065
Volume SD Range			**0.003 – 0.013**		**0.001 – 0.009**	
Group mean volume Healthy			**0.210 ± 0.020**		**0.218 ± 0.022**	
9/59/F/ COPD	67	64	0.345 ± 0.009	14420	0.345 ± 0.001	17518
10/49/M/COPD	69	71	0.320 ± 0.003	14680	0.322 ± 0.002	17960
11/55/F/ COPD	40	61	0.316 ± 0.004	18163	0.316 ± 0.002	19720
12/50/F /COPD	59	58	0.268 ± 0.006	16002	0.269 ± 0.006	19936
13/57/F/ COPD	48	44	0.437 ± 0.001	11767	0.437 ± 0.006	14694
14/58/F/ COPD	63	59	0.294 ± 0.006	15435	0.296 ± 0.007	20222
15/53/F /COPD	55	59	0.374 ± 0.009	16988	0.373 ± 0.002	23888
16/53/M /COPD	56	47	0.340 ± 0.002	22126	0.349 ± 0.006	28838
17/64/M /AATD	65	66	0.353 ± 0.007	15151	0.358 ± 0.007	19888
18/67/M /AATD	69	69	0.449 ± 0.009	15052	0.453 ± 0.011	19645
19/60/F /AATD	72	62	0.384 ± 0.019	14621	0.406 ± 0.003	19626
20/69/F /AATD	62	75	0.385 ± 0.021	14700	0.382 ± 0.003	17918
21/62/F /AATD	45	55	0.434 ± 0.041	11705	0.504 ± 0.008	15309
22/65/M/ AATD	77	66	0.473 ± 0.018	14399	0.465 ± 0.009	18138
23/61/M/ AATD	44	62	0.479 ± 0.007	17004	0.505 ± 0.007	23329
24/56/M/ AATD	51	60	0.440 ± 0.034	20659	0.436 ± 0.008	26055
Volume SD Range			**0.001 – 0.041**		**0.001 – 0.011**	
Group mean volume Patients			**0.381 ± 0.066**		**0.387 ± 0.072**	

FEV_1: forced expired volume in one second. FVC: forced vital capacity. TLC: total lung capacity. ADC: apparent diffusion coefficient. SD: standard deviation. Y: years old

Table 2. Demographic data. Overall mean ADC per subject (mean of three measurement days) with SD at 6% and 15% of TLC shows the intra-individual reproducibility. Group mean calculated as Mean of overall mean ADC per subject with SD shows the inter-individual variation in each group. Number of voxels.

Table 3. Results of the mixed model analysis of overall mean ADC and SD.

		Mean ADC[1]		SD[2] ADC	
	Effect	F-value	p-value	F-value	p-value
Emphysema group	Day	0.94	0.403	0.41	0.669
	Volume	6.26	0.027	3.96	0.068
	Day x Volume	1.63	0.216	0.10	0.905
Healthy group	Day	1.91	0.185	2.71	0.102
	Volume	26.20	0.001	19.35	0.003
	Day x Volume	1.27	0.312	1.52	0.252

[1]ADC: apparent diffusion coefficient. [2]SD: standard deviation.

Table 4. Anterior-posterior mean ADC at 15% of TLC and in the healthy volunteers group. *(ADC: apparent diffusion coefficient. TLC: total lung capacity)*

Healthy subjects	Anterior slices	Posterior slices	Gradient
1	0.224	0.173	0.051
2	0.262	0.195	0.067
3	0.207	0.171	0.036
4	0.264	0.196	0.068
5	0.224	0.179	0.045
6	0.247	0.202	0.045
7	0.242	0.178	0.064
8	0.304	0.210	0.094
Group	0.247	0.188	0.059

Table 5. Anterior-posterior mean ADC at 15% of TLC and in the patient groups.
(ADC: apparent diffusion coefficient. TLC: total lung capacity)

Subjects	Anterior slices	Posterior slices	Gradient
1 COPD	0.320	0.323	-0.003
2 COPD	0.394	0.218	0.176
3 COPD	0.353	0.286	0.067
4 COPD	0.252	0.242	0.010
5 COPD	0.355	0.469	-0.114
6 COPD	0.280	0.270	0.010
7 COPD	0.325	0.378	-0.053
8 COPD	0.328	0.363	-0.035
9 A1AT	0.393	0.291	0.102
10 A1AT	0.542	0.365	0.177
11 A1AT	0.460	0.349	0.111
12 A1AT	0.442	0.381	0.061
13 A1AT	0.500	0.607	-0.107
14 A1AT	0.416	0.422	-0.006
15 A1AT	0.574	0.474	0.100
16 A1AT	0.509	0.404	0.105

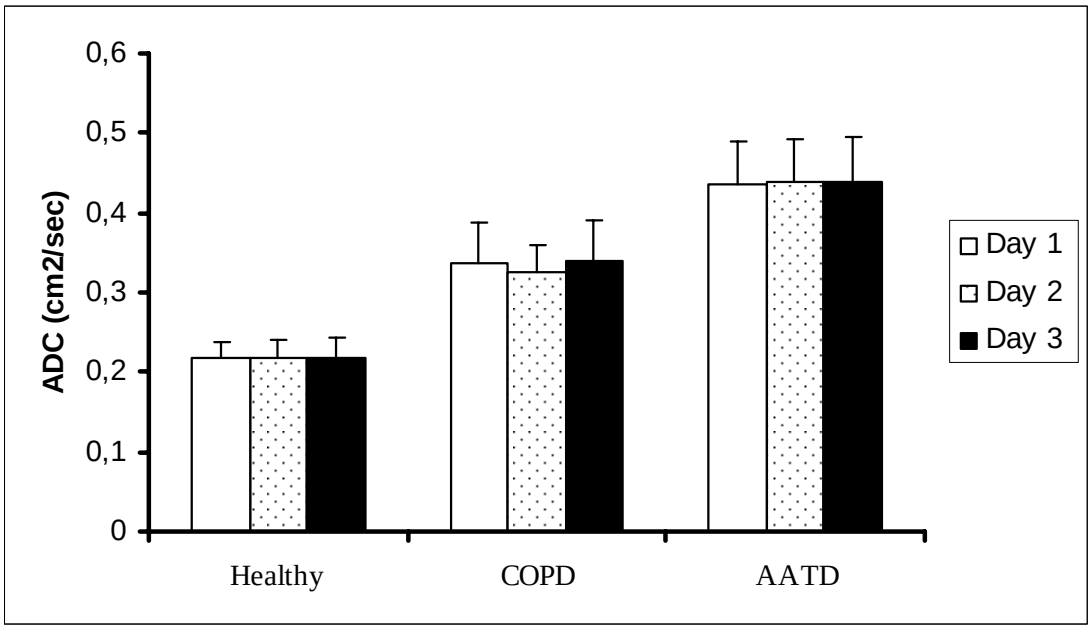

Figure 1. Group Mean ADC at each imaging day at the larger volume (15% of TLC) for all subjects in each group. The error bars represent the standard deviation of the three measurements on three separate days. Note the clear discrimination between the healthy volunteers and the patients.

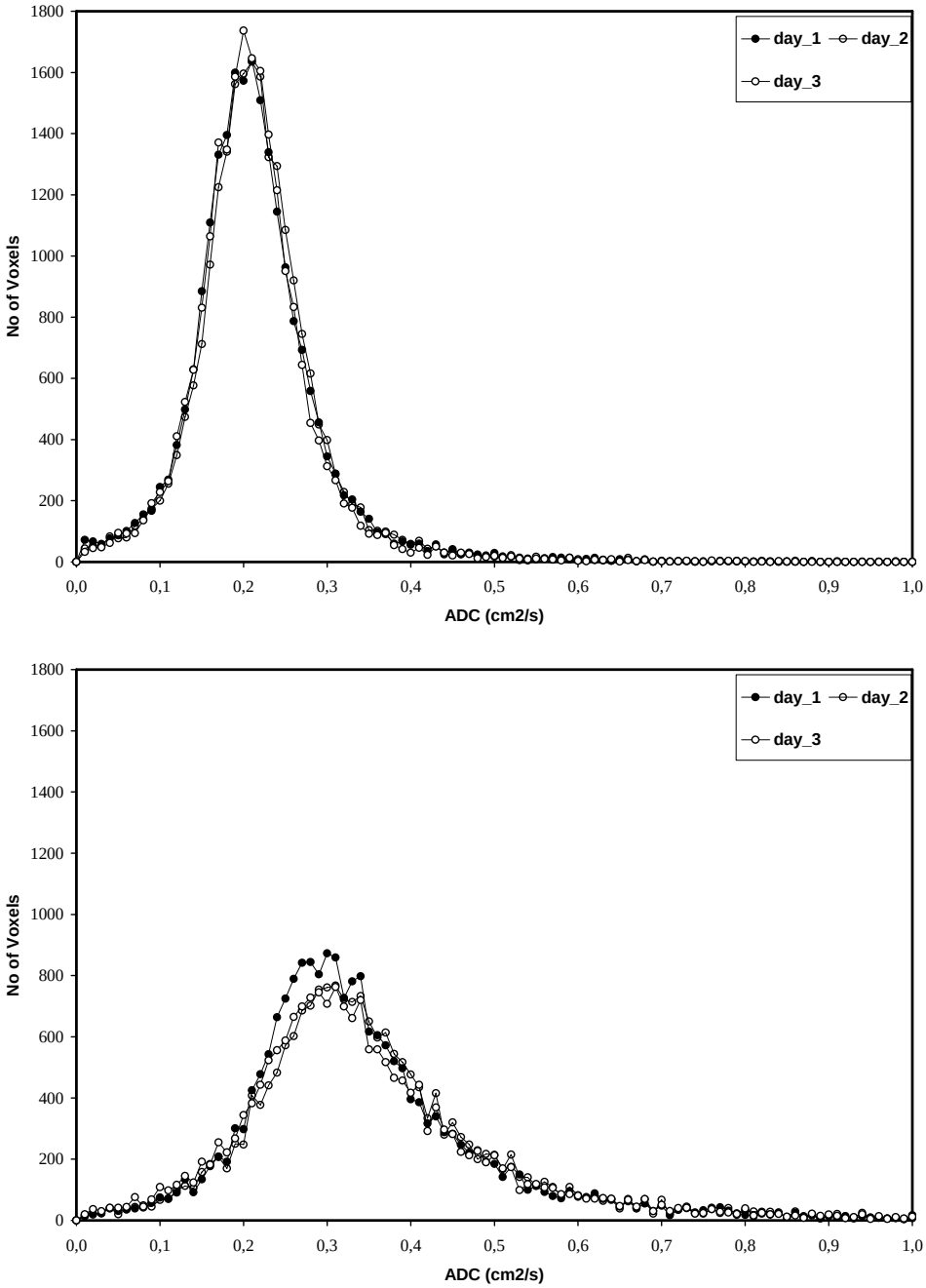

Figure 2. Frequency distribution (No. of voxels versus Mean ADC per subject) at 15% of TLC. *Upper*: one healthy volunteer over three days. *Lower*: one patient over three days. Note the almost identical distribution curves at the different imaging sessions. Note also the difference in the shape of the curve between the volunteer and the patient.

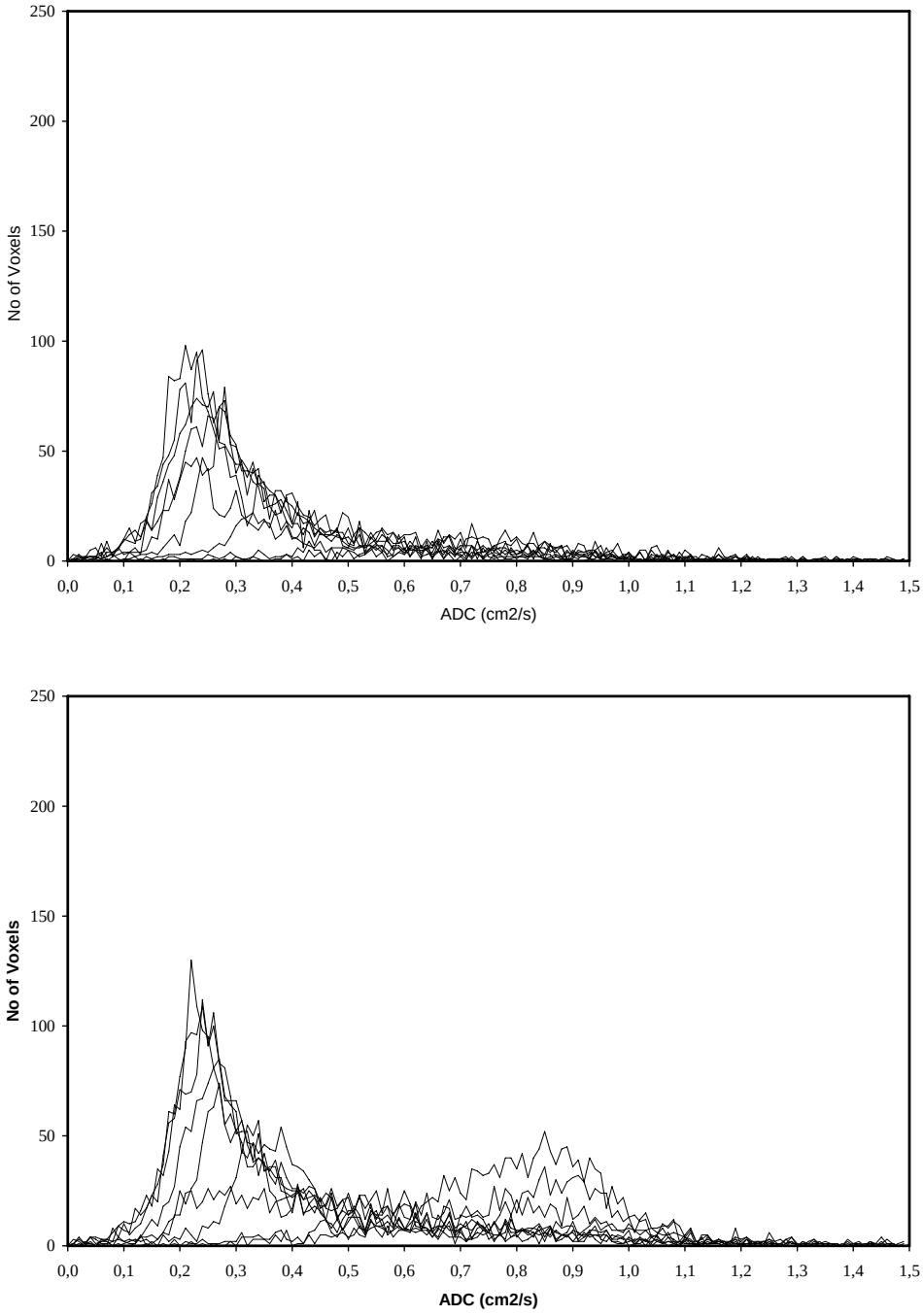

Figure 3. *Above:* Frequency distribution of the 10 slices and ADC maps in one patient (nr. 14) at 6% of TLC. Note the distribution with only one low peak with almost normal mean ADC.

Below: The same patient at 15% of TLC. Note the distribution with two peaks. The high ADC peak represents the emphysematous parts of the lungs, which were not filled with gas at the lower volume.

FIGURE AND LEGENDS

Figure 1. Group Mean ADC at each imaging day at the larger volume (15% of TLC) for all subjects in each group. The error bars represent the standard deviation of the three measurements on three separate days. Note the clear discrimination between the healthy volunteers and the patients.

Figure 2. Frequency distribution (No. of voxels versus Mean ADC per subject) at 15% of TLC. *Above*: one healthy volunteer over three days. *Below*: one patient over three days. Note the almost identical distribution curves at the different imaging sessions. Note also the difference in the shape of the curve between the volunteer and the patient.

Figure 3. *Above:* Frequency distribution of the 10 slices and ADC maps in one patient (nr. 14) at 6% of TLC. Note the distribution with only one low peak with almost normal mean ADC.

Below: The same patient at 15% of TLC. Note the distribution with two peaks. The high ADC peak represents the emphysematous parts of the lungs, which were not filled with gas at the lower volume.